tvst

Refractive Intervention

FIAT: A Device for Objective, Optical Measures of Accommodation in Phakic and Pseudophakic Eyes

Austin Roorda[1], Pavan Tiruveedhula[1], Ayman Naseri[2,3], Paul Rhee[2], and Matt Clarke[2]

[1] University of California at Berkeley, Berkeley, CA, USA
[2] ForSight VISION6, Inc. South San Francisco, CA, USA
[3] University of California, San Francisco, San Francisco, CA, USA

Correspondence: Austin Roorda, 485 Minor Hall, University of California, Berkeley, Berkeley CA 94720-2020, USA. e-mail: aroorda@berkeley.edu

Received: September 10, 2022
Accepted: November 22, 2022
Published: January 6, 2023

Keywords: accommodation; wavefront sensing; instrumentation

Citation: Roorda A, Tiruveedhula P, Naseri A, Rhee P, Clarke M. FIAT: A device for objective, optical measures of accommodation in phakic and pseudophakic eyes. Transl Vis Sci Technol. 2023;12(1):9, https://doi.org/10.1167/tvst.12.1.9

Purpose: To present FIAT, a novel optical instrument and analysis package that is designed to elicit and optically record accommodation in human eyes.

Methods: FIAT employs a Shack-Hartmann wavefront sensor and a retro-illumination pupil camera that records from a single eye at video rates. It is effective at eliciting accommodation by offering the subject a full-field binocular view of an alternating distant target and a near-eye display. FIAT analysis software computes wave aberrations for each video frame over full- or subpupil sizes and computes accommodative dynamics and accommodative range.

Results: The system is validated by showing accurate refraction measurements in model eyes and human eyes with trial lenses. Robust accommodative responses are shown for young eyes, and a lack of accommodative response is shown for a known presbyopes. Accommodative stimulus–response curves from five phakic subjects over a range of ages show expected results. Results from two individuals with monofocal intraocular lenses are shown.

Conclusions: FIAT is an effective instrument for making accurate, objective measures of accommodation in phakic and pseudophakic eyes.

Translational Relevance: We present a device that can play an important role in the development and testing of accommodating intraocular lenses.

Introduction

The refractive state of an eye is defined by the position of an object relative to that eye that casts the sharpest retinal image. It is commonly measured in diopters, which is the inverse of the distance (in meters) from the eye to that object. Accommodation is defined as the ability to change the refractive state of the eye via a physiologic change in the eye's optics[1] to enable focusing on objects at different distances. Accommodation is also commonly measured in units of diopters. The range of accommodation is the difference in diopters between the far point of the eye (the eye's refractive state when it is in it most relaxed state or focused at distance) and its refractive state when maximally accommodated. In a young eye, the range of accommodation can be over 10 diopters (D).[2] The accommodative range is often measured subjectively, but there is a growing desire and need for automated, objective means to accurately measure it.[3]

If the eye were diffraction limited (i.e., free of aberrations), then its refractive state could be computed directly from its power and axial length. Consequently, the range of accommodation could be computed directly from its change in power. However, the eye is not close to diffraction limited but is fraught with aberrations.[4] Moreover, many modern ophthalmic interventions intentionally add aberrations (extended depth of focus lenses) or employ multifocal optics that take the eye even further from being diffraction limited. In these situations, the determination of the refractive state is far more complex and remains an area of active research. Objects placed at a "far point" that is computed from the best-fitting defocus to the complex

wavefront arising from such complex optical systems rarely correspond to the location where the subject deems it to be in best focus.[5–7] What has emerged over the past two decades is that the placement of objects at distances that appear sharpest to the subject corresponds to locations for which image sharpness metrics like Strehl ratio[8,9] or visual Strehl ratio[10,11] are maximized.

Improved insights into the relationships between wave aberration and perceived best focus were made possible through accurate measurements of the wave aberrations of the eye using wavefront sensors.[12] Today, ophthalmic wavefront sensor systems are commercially available and appear to optimize image-sharpness metrics using undisclosed algorithms to provide objective measures of the eye's refractive prescription (Visionix, Luneau Technology, France; Pentacam AXL Wave, Oculus, Arlington, WA, USA[13]; Wavedyn, Wavefront Dynamics, Albuquerque, NM, USA). The use of wavefront sensors to offer objective measures of accommodation is less common (commercial devices: Osiris, CSO Ophthalmic, Scandicci, Italy[14]; COAS-HD, Wavefront Sciences [no longer commercially available][15]; iTrace, Tracey Technologies, Houston, TX, USA[16]; and several reported research devices[17–20]). In essence, the measurement of accommodation effectively involves a measurement of the refractive state of the eye while the subject focuses at difference distances. But that simple difference is more complicated than one might think: aberrations change,[17] the pupil constricts,[21] and the eyes converge[22] with accommodation. Accommodation also fluctuates over time.[23] Finally, accommodation is voluntary, and so it must be elicited in order to be measured.

A recent study using a wavefront sensor compared four different objective metrics to quantify accommodation.[24] Importantly, they compared those objective measures against careful subjective estimates of the accommodative state of the eye in the same apparatus. As in the studies of refractive errors cited above, they found that the objective metrics that correlated best with subjective estimates of accommodation were the Strehl ratio and visual Strehl ratio image sharpness metrics.

Based on the findings described above, we present a device and an approach to quantify accommodation as the magnitude of the shift in the eye's far point as assessed by the Strehl ratio image quality metric. Although the visual Strehl ratio has been found to correlate better with subjective image quality in normal eyes in the unaccommodated state than the Strehl ratio, it does not appear to offer any more accuracy for accommodation measurements,[24] and so we opt to use the more conventional Strehl ratio metric here. More details on the method to quantify the amplitude of accommodation are described in a later section. The methods and results in this report follow the guidance provided by American Academy of Ophthalmology Task Force on how best to demonstrate objective, optical assessments of accommodation.[25]

Methods

FIAT System

FIAT (ForSight Intraocular lens Accommodation measurement Technology) is a Shack-Hartmann–based wavefront sensor. The specific features that make FIAT suitable for measuring accommodation are as follows:

1. Frame rates up to 30 frames per second
2. A synchronously recorded retro-illumination pupil image to visualize, identify, and track features in the optics, like lens opacities or structural features in an intraocular lens (IOL)
3. Full-field binocular viewing to elicit maximum accommodation
4. A physical, high-resolution near-eye display connected to a servo-motor that can be used to flip the display up or down as desired. The display is presented along the line of sight of the measured eye but is visible to both eyes. The near-eye display can be positioned anywhere along a linear track to present at distances ranging from 100 to 30 cm (1 to 3.33 D stimulus to accommodation)
5. A novel analytical approach to compute the amplitude of accommodation based on image sharpness metrics (see Analysis section)

The rationale and consequent advantages of the system with these combined features will be revisited in the Discussion. A Solidworks (Dassault Systemes, Vélizy-Villacoublay, France) rendering of the system with and without the enclosure and near-eye display is shown in Figure 1.

To ensure high fidelity of sampling over the crystalline lens or over a more complex IOL, FIAT employs a high-density, square lenslet sampling array with 112.5-µm pitch in the pupil plane. This is achieved with a lenslet array with a 150-µm pitch (MLA150-7AR; Thorlabs, Newton, NJ, USA) and magnification of 0.75 in the telescope relaying the pupil of the eye to the lenslet array. The measurement

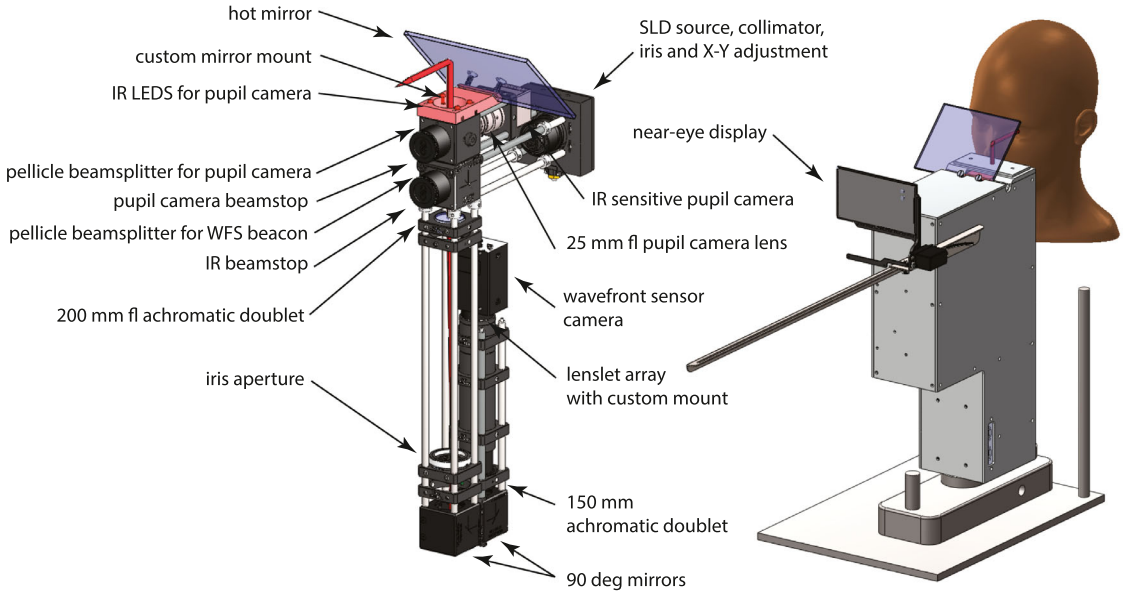

Figure 1. FIAT system. The *left panel* shows the system with the main parts labeled. The *right panel* shows the system with the enclosure and with the near-eye display in the up position. Note that when the display is up, it is readily visible through the hot mirror with both eyes. When the display is down, the subject gets an unimpeded binocular view of distant targets through the hot mirror.

is made with an 875-nm superluminescent diode (model: L11607-04; Hamamatsu Photonics, Shizuoka, Japan) as a laser beacon to provide ample signal while minimizing the subject's visibility of the wavefront sensor beacon during the accommodation task. The average power at the eye from the laser beacon is <10 µW. An adjustable aperture is placed at the common focal point in the telescope of the system. This aperture is used to minimize ambient light, scattered light, and reflections from the eye's optics from reaching the wavefront sensor and contaminating the measurement. This aperture limits the dynamic range of the system to about ± 3.5 D. If a larger dynamic range is desired, it can be increased by opening the aperture at the expense of measurement noise caused by increased back reflections from the eyes optics.

The camera used for the retro-illumination image is an infrared (IR)-sensitive monochromatic CMOS camera (UI-3860CP-M/C; IDS Imaging, Woburn MA, USA). The retro-illumination image is derived from the same light source as the wavefront sensor. A conventional image of the eye and pupil with forward illumination can also be viewed by switching on a set of four IR LEDs mounted near the hot mirror (Fig. 1).

The FIAT system can also be equipped with hardware to measure model eyes or any type of lens outside of the eye, including IOLs. In this mode, the hot mirror is replaced with a regular mirror that directs the measurement beam through an optomechanical chassis that is configurable for a multitude of different tests. For system validation, the model eye could be a diffraction-limited lens with a distance-adjustable retina comprising a single diffuse-reflecting surface. Or, for ex vivo IOL measurements, for example, a high-power lens can be used to simulate the cornea, the IOL can be placed in a water-filled cuvette immediately behind the lens, and a piece of diffusely scattering paper can be placed at the focal point of the lens assembly to simulate the retina.

Measurement Procedure

The measurement procedure involves simultaneous recording of video from a Shack-Hartmann wavefront sensor and a retro-illumination pupil camera. During the recording, either the near-eye display is presented or it is flipped down for distance viewing. The timing of the presentation of the near-eye display and the length of the recording can be programmed by the operator.

Anything can be presented on the displays. For the measurements in this report, a set of five-letter words was presented as white on a black background. In order to elicit maximum accommodation, the letter size on the near-eye display was adjusted by the operator to find a size that was deemed to be just readable by the subject.

The raw data consist of a single digital video where the wavefront sensor and the retro-illumination video frames are shown side-by-side. A single frame adapted from a representative video sequence is shown in Figure 2.

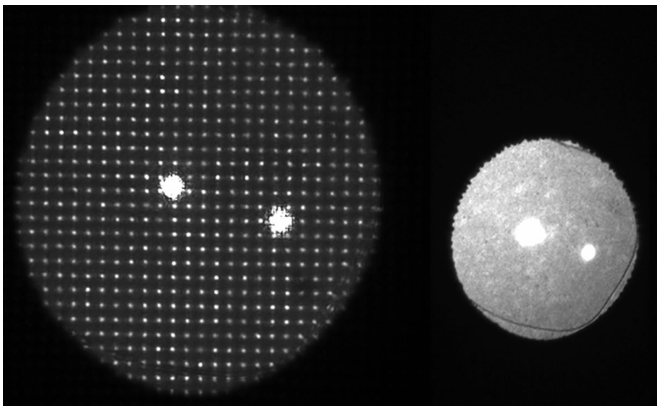

Figure 2. Raw, single-frame images from the FIAT system from subject IOL-S1. The *left frame* shows the Shack-Hartmann wavefront sensor image, and the *right frame* shows the retro-illumination pupil image of the same eye acquired at the same time. The scales are different. For this subject, who has a monofocal IOL implant, the retro-illumination image reveals some features of the capsulorhexus boundaries.

Analysis

The output data are analyzed offline in two stages using custom software.

Video Processing

The first stage is the video processing. In this stage, the operator can decide on a number of options: (1) analyze all the Shack-Hartmann spots across the changing pupil size over the course of the entire video or (2) track the full pupil but analyze spots over a fixed subpupil that is centered on the anatomic pupil.

In all scenarios, the operator can choose to generate a wavefront fit with either a 10th-order Zernike polynomial (65 terms) or a 6th-order Zernike polynomial (27 terms) ordered according to the Optical Society of America standard for vision science.[26] A lower-order fit is recommended for smaller pupils.

The output of this stage is a video like Figure 2 but with the Shack-Hartmann centroids overlaid on the wavefront sensor image and a text file that tabulates all primary metrics from each frame (max pupil size, analyzed pupil size, root-mean-square (RMS)-based estimates of refractive error, and the Zernike polynomial coefficients).

Extended Analysis

In this stage, the outputs from the video processing stage are used to compute a series of metrics from the video traces, specifically related to accommodation. At the onset, the operator can decide on a few options, including a decision to either process the wavefronts directly from the video processing stage (i.e., use the same pupil size for which the Zernike coefficients were generated) or process data using a fixed subpupil. The extended analysis involves the following analyses for each video frame.

1. Correct for the chromatic difference of refraction of 1.00 D between the measurement wavelength (875 nm) and wavelength for peak sensitivity (555 nm).[27] We note that there is individual variability in the chromatic aberration of the eye, and so the exact refractive state of the eye might be variable. This variability will offset the traces of refractive state but will not affect the amplitude of accommodation.
2. Compute and display the wave aberration map.
3. Compute the best-fitting defocus from the wavefront (corresponding to Zernike coefficient 4). Incidentally, this best-fitting sphere also corresponds to the spherical equivalent defocus.
4. Compute a series of through-focus point spread functions (PSFs) over a user-defined defocus range and resolution (e.g., –3 D to +1 D in 0.2-D steps).
5. Convolve a Snellen E of a user-defined size (e.g., 20/20) with each of the through-focus PSFs and display each image in line with the bar graph in step 6.
6. Compute the Strehl ratio for each of the through-focus settings and display as a bar graph.
7. Plot a chart record with three traces: the dioptric position of the near-eye display, the RMS defocus, and the defocus that optimizes the Strehl ratio.

An example screenshot from the FIAT extended display window is shown in Figure 3. In this instance, the analysis was of a recording over a 3-mm subpupil from a 38-year-old subject with typical levels of accommodation.

Quantification of Accommodation

Here we define how the accommodative range is computed. As shown in Figure 3, the aberrations of the eye and consequent defocus estimates are reported at 30 Hz. Considering measurement noise, it is inappropriate to compute accommodative range as the peak to valley of the defocus trace however computed, since a noisier measurement would erroneously yield a larger range. Additionally, a brief moment of accommodation, even if it did occur, might not be sufficiently sustained for the subject to perform optimally on a near-vision task. Considering these two points, we opted to compute accommodation from a running average of the defocus state over a 400-ms period (12 frames at 30 fps); 400 ms was chosen since it is the duration time required to achieve optimal

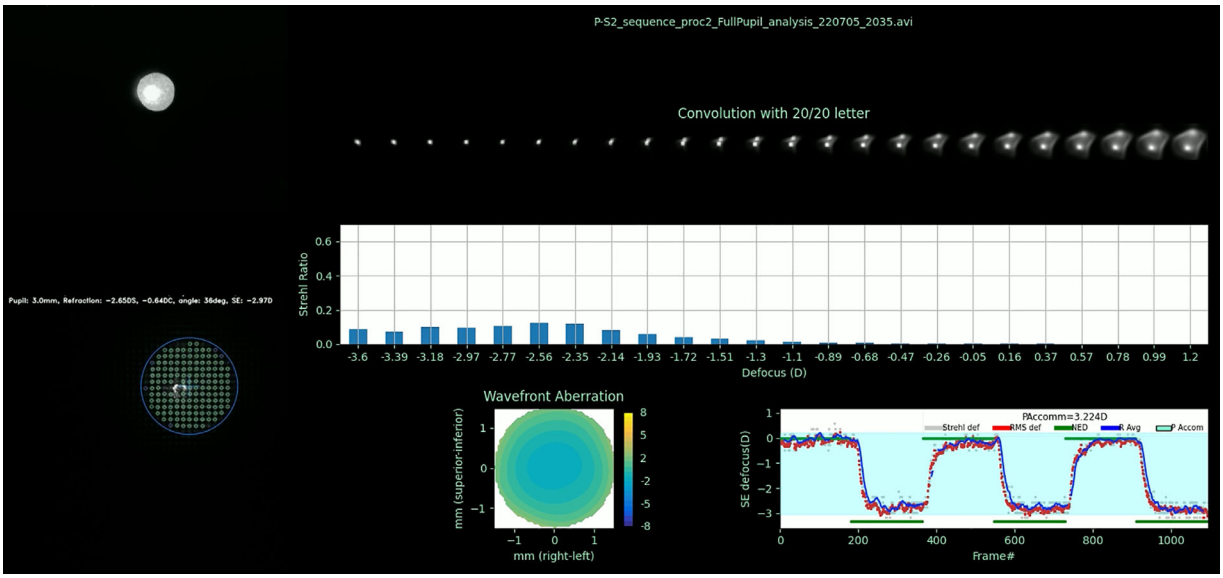

Figure 3. Final frame from the FIAT extended analysis from subject P-S2.

acuity.[28] After computing the running average, the accommodative range was taken as the difference between the highest sustained refractive state when the distant display was presented and the lowest sustained refractive state when the near-eye display was presented. Neither the maximum nor the minimum were computed for a period of 1 second following when the near or distance display was shown to account for accommodative latency. For all the analyses in this report, unless otherwise specified, the accommodative range is a single value computed from a single video sequence, where a single video sequence comprises three presentations of the near-eye display (see Fig. 3).

Human Subjects

Data from five phakic eyes were collected for the sole purpose of the present study at ForSight VISION6 labs, designated P-S1 to P-S6. Data from five pseudophakic eyes with monofocal IOLs were collected for part of a nonrelated clinical trial being performed in Mexico City, designated IOL-S1 to IOL-S5. Informed consent was obtained from all subjects prior to data collection. Both studies were approved by an ethics committee, and research procedures followed the tenets of the Declaration of Helsinki. For one of the phakic eye measurements done at the ForSight VISION6 location, the subject (P-S1) was administered a single drop of 2.5% phenylephrine to facilitate wavefront measurements over the largest pupil possible during accommodation.

Results

Validation in a Model Eye

A first validation for FIAT was to measure refraction of a model eye with a distance-adjustable lens. The model used an achromatic doublet lens (part ACL254-100B from Thorlabs) and a diffusely scattering retina (paper) whose position relative to the lens could be carefully controlled with a micrometer. The published physical properties of the lens (focal length, chromatic aberration, back vertex focal length) were used to compute the expected defocus for each distance setting. A range of distances spanning the intended dynamic range of the system was generated. Figure 4A shows a plot of the measured versus expected results. The changes are highly linear, and the slope is close to 1, which means that the system measures the defocus precisely and accurately.

Validation in Humans

Although a model eye may behave as expected, data collected on a living human eye might be noisy, or other unknown factors could bias the results. For this validation, two monofocal IOL subjects IOL-S2 and IOL-S3 were positioned in the instrument, and +1-D, +2-D, and +3-D trial lenses were periodically placed in front of their eye to simulate a known refractive error. Expected powers were the effective powers, which were computed considering a vertex distance of 25 mm between the trial lens and the entrance pupil of the eye

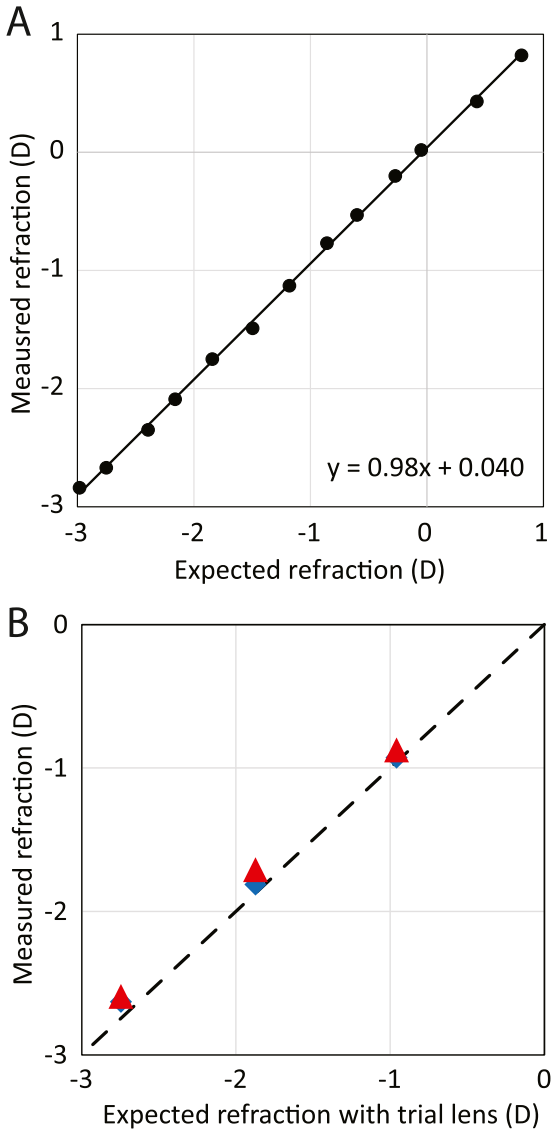

Figure 4. FIAT validation on model and human eye. (A) Measured v.s. expected defocus for a model eye in the FIAT system. The equation shows the slope and intercept of the best fit. (B) Measured v.s. expected defocus for trial lenses placed in front of two monofocal pseudophakic subjects, IOL-S2 and IOL-S3. The *symbols* indicate values measured from the two subjects, and the *dashed line* indicates the expected value.

as well as the difference in lens power between visible (555 nm) and near infra-red (875 nm) wavelengths of the FIAT wavefront sensor. Figure 4B plots the results from both subjects. Over a 3-D operating range, the average departure from expected was just over 0.1 D.

Justification for Using Peak Strehl Ratio as a Criterion for Best Focus

Figure 5 shows the output of a FIAT measurement sequence with three alternating presentations of a target at distance and a near target at 3.33 D. The subject was a 35-year-old man (subject P-S1) with no refractive error. For this specific measurement, the subject had one drop of 2.5% phenylephrine, which minimized the pupil constriction, although it still varied by ≈1 mm over the course of the measurement. The defocus coefficient changed systematically with the near and distance targets, as expected. When the eye was relaxed, there was significant positive spherical aberration, but it showed the expected shift toward negative whenever the defocus increased.[17] For the defocus analysis in Figure 6, the entire pupil was analyzed for each frame. The entire movie sequence is included in the Supplementary Materials. The figure shows a clear departure between the defocus estimate based on the best-fitting sphere to the wavefront (RMS-based defocus) and the defocus that optimizes the image sharpness (Strehl-based defocus). The RMS-based defocus suggests that the eye is myopic or overaccommodated on the distant target, whereas the Strehl defocus estimate indicates that the eye is well focused for the distance target. The disparities are especially evident for the distant target because this is where the spherical aberration is most positive. The presence of monochromatic aberrations, particularly spherical aberration, is known to render RMS-based estimate

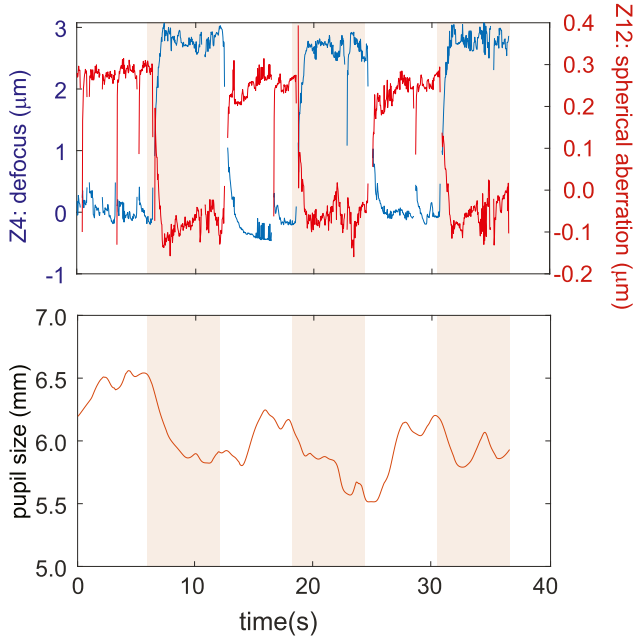

Figure 5. Defocus (*blue trace*) and spherical aberration (*red trace*) Zernike coefficients for a 35-year-old phakic eye (subject P-S1) viewing three sequential presentations of a near-eye display at 3.33 D, indicated by *shaded regions*. The coefficients are computed over the full pupil (*lower plot*). The plots show that with the near-eye display, the pupil constricts slightly, the defocus increases, and the spherical aberration goes from positive to negative.

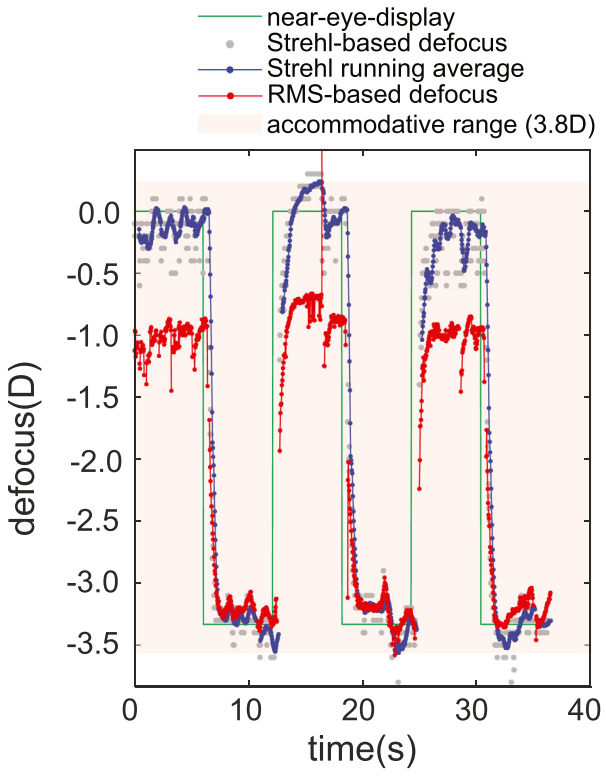

Figure 6. FIAT extended analysis sequence for a 35-year-old phakic eye (subject P-S1) viewing three sequential presentations of a near-eye display at 3.33 D. The Strehl-based defocus estimates (*gray symbols*) are based on a computation of the Strehl ratio at each 0.1-D discrete defocus step. As such, the *gray symbols* are quantized at a 0.1-D resolution for each frame (similar step sizes are used for the calculations in subsequent figures). The defocus is computed over the full pupil for each frame. The plot reveals a 3.8-D accommodative range, based on the Strehl ratio.

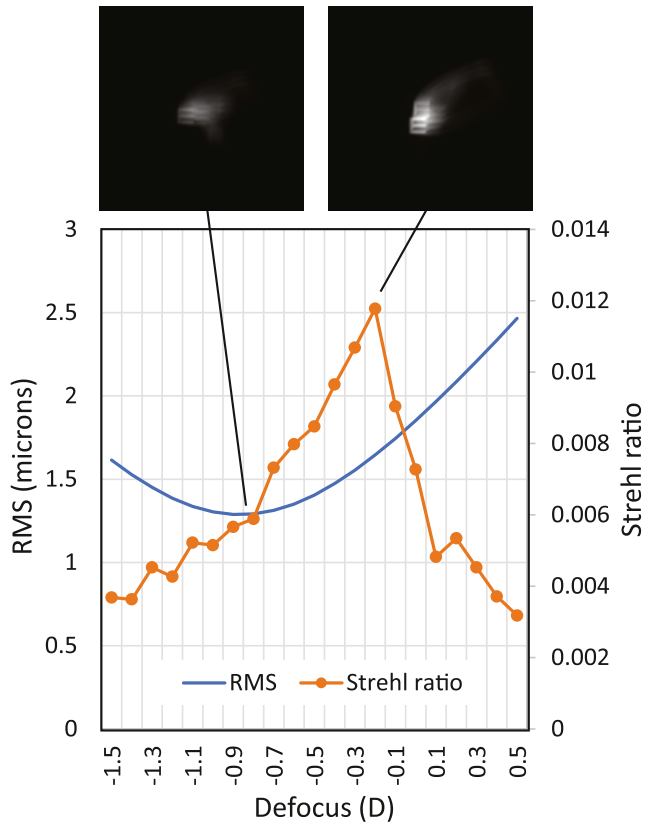

Figure 7. Plot of through-focus RMS and Strehl ratio for one of the frames from the sequence in Figure 6. A 20/20 E (5 arcmin height) convolved with the PSFs at minimum RMS and maximum Strehl is shown. The pixel intensities are scaled by the relative Strehl ratio between the two defocus states.

defocus less accurate.[5,6] We note here that the subject has never required spectacles to correct his distance vision.

Further support for the Strehl-based approach to computing defocus is shown in Figure 7. We took a single frame from the sequence and performed a through-focus analysis to compute the Strehl ratio and the RMS from –1.5 D to 0.5 D. The plot shows that the Strehl ratio peaks at a defocus of –0.2 D, whereas the RMS is a minimum at –0.8 D. The images show convolved 20/20 letters with the PSF at each of the two minima. Owing to the presence of significant aberrations for this 6.5-mm pupil, neither image is sharp, but the E in the convolved image at the peak Strehl has higher contrast and is more legible.

Phakic Human Eyes

Figure 8 shows the results from two phakic subjects computed over a 3-mm pupil. The top panel is from a 38-year-old subject (P-S2) with normal accommodation. In that case, a very typical accommodative pattern is found and the focal plane tracks the stimulus very well. Overall accommodative range was 3.19 D for a 3.33-D stimulus. The second panel is from a 55-year-old subject (P-S4), self-reported to be presbyopic, who exhibits virtually no accommodation for a 2.5-D stimulus.

Accommodative Response Curves

For these experiments, measurement sequences similar to those shown in Figure 8 were measured for a series of near-eye display positions at 0 D, 1.5 D, 2.5 D, and 3.33 D. The maximum accommodative amplitude from each sequence was computed. Figure 9 plots the response for nine eyes from five individuals with the following ages: P-S1:35, P-S2:38, P-S3:45, P-S4:55, and P-S5:57. For P-S1 and P-S2, the accommodation is very accurate and does not reveal the often-reported lead and lag of accommodation. This is not surprising for two reasons: first, FIAT looks for the maximum sustained accommodation response over

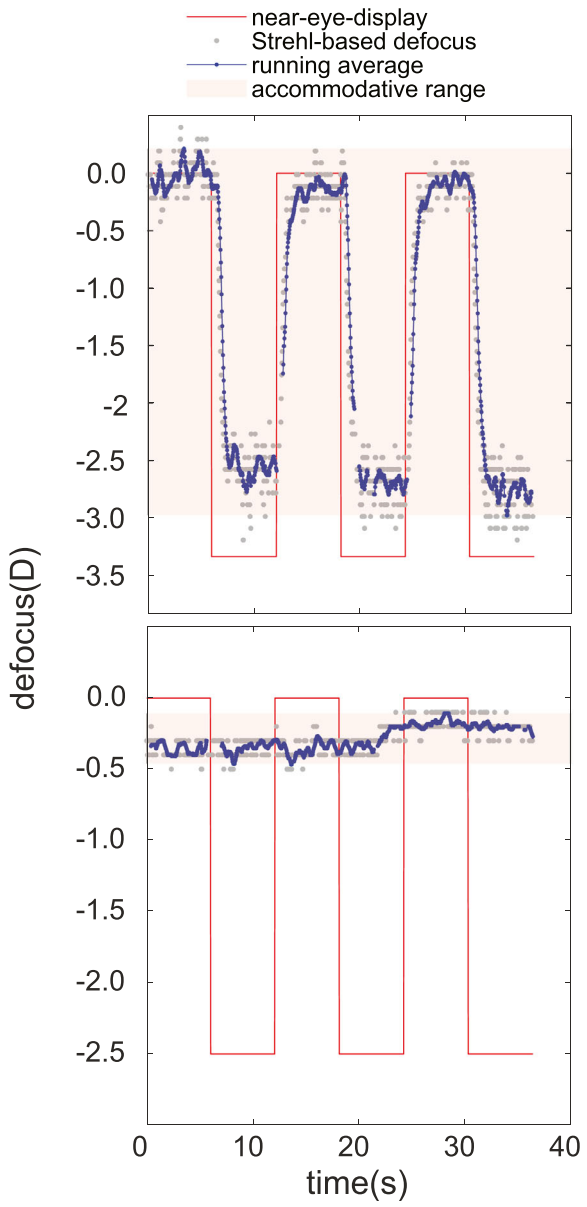

Figure 8. FIAT traces from two eyes. The refractive state in both traces is computed from a 3-mm subpupil centered on the physiologic pupil. The *upper trace* is from a 38-year-old eye (P-S2) responding to three cycles of a near-eye display at 30 cm (3.33-D accommodative demand). The *lower trace* is from a 55-year-old presbyope (P-S4) who exhibits virtually no accommodation to a display at 40 cm (2.5-D accommodative demand).

the course of three near-eye display presentations in a sequence. Second, the Strehl ratio–based method to compute the refractive error and consequent accommodation has been recently shown to provide accommodative response curves with less lead and lag.[24] P-S2 revealed about 1 D of myopia in their right eye, and the sustained "overaccommodation" suggests that the accommodative response was likely driven

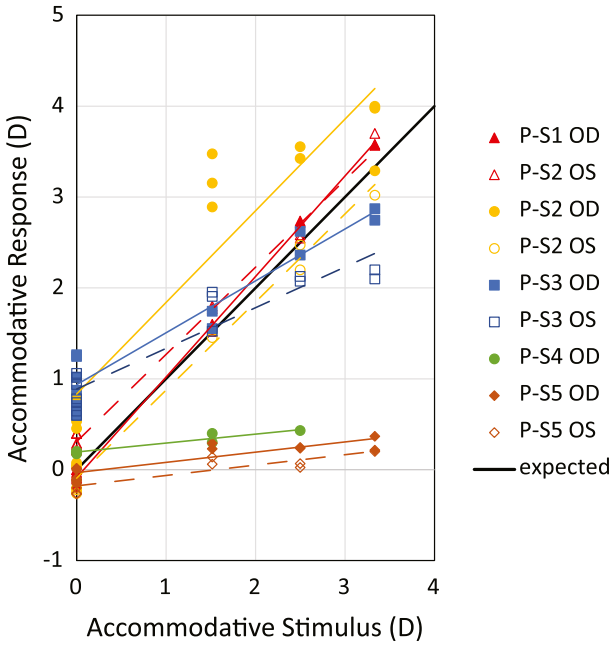

Figure 9. Accommodation stimulus–response curve for the five phakic subjects. The younger emmetropic eyes show excellent responses to the stimuli.

by the left eye. P-S3 was also about 1 D myopic and, being 45 years old, exhibited an expected limited range of accommodation. Finally, P-S4 and P-S5 both showed essentially no accommodation, indicating presbyopia.

Human Eyes With Monofocal, Nonaccommodating IOLs

Figure 10 shows results from two subjects, IOL-S4 and IOL-S5, who were implanted with monofocal IOLs. In both cases, there is some variability in the defocus, suggesting some apparent accommodative effort, but only 0.36 D and 0.3 D were observed as per the definition.

Discussion

In this report, we demonstrate FIAT to be an effective tool for measuring accommodation in eyes with natural and artificial lenses. FIAT combines a unique set of optics and software analysis that makes it uniquely suitable to measure accommodation, especially for future applications to evaluate accommodating IOLs (A-IOLs). These features are discussed here.

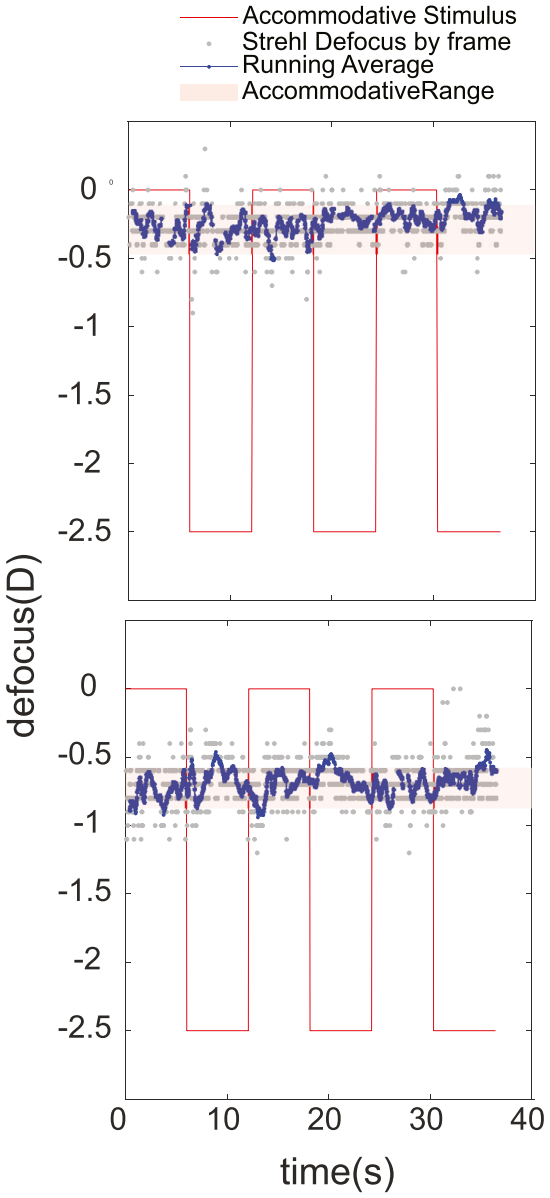

Figure 10. Trace from two subjects with monofocal IOLs (subjects IOL-S4 and IOL-S5). In both cases, the wave aberration was measured over a fixed 2.4-mm subpupil centered on the actual pupil. There is some variability in the defocus perhaps due to some accommodative effort shifting the lens, but no systematic accommodation is evident when presented with the near-eye display.

High Frame Rates

The current system is set up to run at 30 Hz. This rate is set to be slow enough to maximize light collection per frame yet is sufficient to capture changes in accommodation. If higher frame rates are desired (e.g., to measure accommodative fluctuations), they could be achieved with software and hardware modifications.

Synchronous Retro-Illumination Pupil Image

This feature offers sharp images of scattering features and opacities in the lens that are beyond the resolution limit of the wavefront sensor. As an example, the retro-illumination pupil image can resolve and identify distinct features of the capsulorhexus in Figure 2. In future applications, the feature might be used to identify and resolve features inherent to any A-IOL or multifocal IOL design. Although other wavefront sensors offer a pupil/eye camera (e.g., COAS-HD),[15] to our knowledge, no other system has reported on the use of a retro-illumination pupil camera. Note that FIAT also has IR LEDs to use the pupil camera in direct-illumination mode (see Fig. 1).

Full-Field Binocular Viewing

As stated in the Introduction, this is an important feature that is essential to elicit maximum accommodative effort. This feature is inspired by a similar full-field view offered by other devices that measure accommodation, such as the SRW-5000 autorefractor (Shin-Nippon Commerce Inc., Tokyo, Japan)[29,30] or the Plusoptix photorefraction system (PowerRef3; Plusoptix, Nuremberg, Germany), although neither of these devices employ wavefront sensors. To our knowledge, the only other wavefront sensing system that offers full-field binocular viewing is the binocular wavefront sensor developed by Kobayashi et al.[19] Commercial wavefront sensors that offer the ability to measure accommodation have less-than-ideal options to stimulate accommodation: they either present a fixation target to one eye within the device whose vergence is adjusted optically (COAS-HD, Wavefront Science; Osiris) or allow free monocular viewing of a near target through a small aperture in the system (iTrace; Tracey Technologies, Houston, TX, USA). We argue that the full-field view is especially important to elicit accommodation, especially in naive elderly patients with A-IOL implants. As can be seen from the results (Fig. 9), the accommodative response for younger eyes is very accurate and, albeit with a small sample, shows little evidence of accommodative lag that is often reported in the literature.

Physical Near-Eye Display

An actual near eye display viewed over its full extent was employed because it contains all the cues that can help to elicit maximum accommodation. The current near-eye display can be positioned on a rail anywhere

from 1 m to 33 cm. Modifications to the hardware could extend this range in either direction if desired.

Unique Analysis Tools

The analysis tools that are used to compute accommodative amplitude and other optical properties of the eye during accommodation are based on years of research to learn how best to convert accurate measures of the wave aberrations into accurate estimates of the refractive state. RMS-based measures of refraction and/or spherical equivalent are relatively easy to compute but are known not to yield reliable estimates of subjective best focus. Image sharpness–based metrics have emerged as the preferred approach, and human subjects generally agree that images appear sharpest when these metrics are maximized.[8–11] Figure 7 shows a clear disparity between RMS and Strehl ratio–based metrics, especially for larger pupils when the aberrations are high. In that analysis, we argue that the Strehl-based metric is almost certainly more accurate as the subject being measured is not 1 D myopic for distance targets. While there are at least two published reports where image quality–based metrics are used to estimate accommodation,[7,24] most use simple[15,19] or more advanced RMS-based metrics[31–33] or do not describe the exact method in their papers or manuals. By decoupling the data acquisition from the analysis, the system offers maximum flexibility, including user settings such as the number of Zernike terms for wavefront fitting and variable pupil sizes for analysis. In addition to the refraction and accommodation, the suite of tools enables analysis of a host of other metrics, some of which are shown in Figure 5.

Aside from the retro-illumination pupil camera, none of the features of FIAT are completely new. Nevertheless, the combination of all of these features is unique and offers an effective tool to measure properties of accommodation in phakic and pseudophakic eyes.

We have completed the steps suggested by the American Academy of Ophthalmology Task Force[25] to validate an approach to objectively and optically measure true accommodative changes in the power of the eye. We confirmed system accuracy with a calibrated, focus-adjustable model eye; we confirmed accuracy of measurements in a human eye by placing +1-D, +2-D, and +3-D trial lenses in front of a nonaccommodating human eye; we measured accurate accommodative responses in a young phakic eye and lack thereof in a known presbyopic eye. Finally, the system is designed to elicit maximum accommodative response, as evidenced by an apparent lack of accommodative lag for accommodative demands as high as 3.3 D.

Conclusion

Supported by the results shown in this report, FIAT is a useful tool for optical, objective measures of accommodation in human eyes, including pseudophakic eyes with monofocal or accommodating IOLs.

Acknowledgments

Disclosure: **A. Roorda**, ForSight Vision6 (C), ForSight Vision6 (P); **P. Tiruveedhula**, ForSight Vision6 (C); **A. Naseri**, ForSight Vision6 (E), ForSight Vision6 (P); **P. Rhee**, ForSight Vision6 (E); **M. Clarke**, ForSight Vision6 (E), ForSight Vision6 (P)

References

1. Glasser A. Restoration of accommodation: surgical options for correction of presbyopia. *Clin Exp Optom*. 2008;91(3):279–295.
2. Charman WN. The eye in focus: accommodation and presbyopia. *Clin Exp Optom*. 2008;91(3):207–225.
3. Thibos LN, Xin H, Bradley A, Applegate RA. Accuracy and precision of objective refraction from wavefront aberrations. *J Vis*. 2004;4(4):329–351.
4. Porter J, Guirao A, Cox IG, Williams DR. Monochromatic aberrations of the human eye in a large population. *J Opt Soc Am A*. 2001;18(8):1793–1803.
5. Cheng X, Bradley A, Thibos LN. Predicting subjective judgment of best focus with objective image quality metrics. *J Vis*. 2004;4(4):310–321.
6. Martin J, Vasudevan B, Himebaugh N, Bradley A, Thibos L. Unbiased estimation of refractive state of aberrated eyes. *Vis Res*. 2011;51(17):1932–1940.
7. López-Gil N, Fernandez-Sanchez V, Thibos LN, Montes-Mico R. Objective amplitude of accommodation computed from optical quality metrics applied to wavefront outcomes. *J Optom*. 2009;2(4):223–234.
8. Guirao A, Williams DR. A method to predict refractive errors from wave aberration data. *Optom Vis Sci*. 2003 1;80(1):36–42.
9. Roorda A. Human visual system-image formation. In: Hornak JP, ed. *Encyclopedia of Imaging*

Science and Technology. New York, NY: John Wiley & Sons, Ltd; 2002:539–557.
10. Marsack JD, Thibos LN, Applegate RA. Metrics of optical quality derived from wave aberrations predict visual performance. *J Vis*. 2004;4(4):322–328.
11. Hastings GD, Marsack JD, Thibos LN, Applegate RA. Normative best-corrected values of the visual image quality metric VSX as a function of age and pupil size. *J Opt Soc Am A*. 2018;35(5):732.
12. Liang J, Williams DR. Aberrations and retinal image quality of the normal human eye. *J Opt Soc Am A*. 1997;14(11):2873–2883.
13. Balparda K, Acevedo-Urrego A, Silva-Quintero LA, Herrera-Chalarca T. The Pentacam AXL Wave provides a reliable wavefront-based objective refraction when compared to manifest subjective refraction: a prospective study. *Indian J Ophthalmol*. 2022;70(5):1533–1537.
14. Singh NK, Jaskulski M, Ramasubramanian V, et al. Validation of a clinical aberrometer using pyramidal wavefront sensing. *Optom Vis Sci*. 2019;96(10):733–744.
15. Mathur A, Gehrmann J, Atchison DA. Influences of luminance and accommodation stimuli on pupil size and pupil center location. *Invest Ophthalmol Vis Sci*. 2014;55(4):2166–2172.
16. Win-Hall DM, Glasser A. Objective accommodation measurements in prepresbyopic eyes using an autorefractor and an aberrometer. *J Cataract Refract Surg*. 2008;34(5):774–784.
17. Cheng H, Barnett JK, Vilupuru AS, et al. A population study on changes in wave aberrations with accommodation. *J Vis*. 2004;4:27280.
18. Kanda H, Kobayashi M, Mihashi T, Morimoto T, Nishida K, Fujikado T. Serial measurements of accommodation by open-field Hartmann–Shack wavefront aberrometer in eyes with accommodative spasm. *Jpn J Ophthalmol*. 2012;56(6):617–623.
19. Kobayashi M, Nakazawa N, Yamaguchi T, Otaki T, Hirohara Y, Mihashi T. Binocular open-view Shack-Hartmann wavefront sensor with consecutive measurements of near triad and spherical aberration. *Appl Opt*. 2008;47(25):4619–4626.
20. Franco S, Gomes J. Real-time measurement of ocular wavefront aberrations in symptomatic subjects. *BioMed Res Int*. 2018;2018:9415751.
21. Stark LR, Atchison DA. Pupil size, mean accommodation response and the fluctuations of accommodation. *Ophthalmic Physiol Opt*. 1997;17(4):316–323.
22. Schor CM. A dynamic model of cross-coupling between accommodation and convergence: simulations of step and frequency responses. *Optom Vis Sci*. 1992;69(4):258–269.
23. Alpern M. Variability of accommodation during steady fixation at various levels of illuminance. *J Opt Soc Am A*. 1958;48(3):193–197.
24. Labhishetty V, Cholewiak SA, Roorda A, Banks MS. Lags and leads of accommodation in humans: fact or fiction? *J Vis*. 2021;21(3):21.
25. Glasser A, Hilmantel G, Calogero D, et al. Special report: American Academy of Ophthalmology Task Force recommendations for test methods to assess accommodation produced by intraocular lenses. *Ophthalmology*. 2017;124(1):134–139.
26. Thibos LN, Applegate RA, Schwiegerling J, Webb RH, Members VST. Standards for reporting the optical aberrations of eyes. In: Lakshminarayanan V, ed. *Vision Science and its Applications. No. 35 in Trends in Optics and Photonics*. Washington, DC: Optical Society of America; 2000:232–244.
27. Atchison DA, Smith G. Chromatic dispersions of the ocular media of human eyes. *J Opt Soc Am A*. 2005;22(1):29–37.
28. Baron WS, Westheimer G. Visual acuity as a function of exposure duration. *J Opt Soc Am A*. 1973;63(2):212–219.
29. Wolffsohn JS, Gilmartin B, Mallen EA, Tsujimura SI. Continuous recording of accommodation and pupil size using the Shin-Nippon SRW-5000 autorefractor. *Ophthalmic Physiol Opt*. 2001;21(2):108–113.
30. Labhishetty V, Cholewiak SA, Banks MS. Contributions of foveal and non-foveal retina to the human eye's focusing response. *J Vis*. 2019;19(12):18–28.
31. Hughes RP, Read SA, Collins MJ, Vincent SJ. Higher order aberrations and retinal image quality during short-term accommodation in children. *Vis Res*. 2021;188:74–84.
32. Iskander RD, Davis BA, Collins MJ, Franklin R. Objective refraction from monochromatic wavefront aberrations via Zernike power polynomials. *Ophthalmic Physiol Opt*. 2007;27(3):245–255.
33. Perez-Merino P, Birkenfeld J, Dorronsoro C, et al. Aberrometry in patients implanted with accommodative intraocular lenses. *Am J Ophthalmol*. 2014;157(5):1077–1089.

Supplementary Material

Supplementary Movie S1. Extended analysis output corresponding to the same sequence shown in Figure 6.